Simulation of Run-out caused by Imperfection of Ball Bearing for High-speed Spindle Units

Igor Aexeevich Zverev[1], In- Ung Eun[2], Won-Jee Chung[3] and Choon-Man Lee[3,#]

1 Department of Machine Tools, Moscow State University of Technology(STANKIN), Moscow, Russia
2 Department of Die and Mold Design, Kyonggi Institute of Technology, Siheung, South Korea
3 Department of Mechanical Design and Manufacturing, Changwon National University, Changwon ,South Korea
Corresponding Author / E-mail: cmlee@sarim.changwon.ac.kr, TEL: +82-55-279-7572, FAX: +82-55-267-5142

KEYWORDS : High-speed spindle unit, Rotational accuracy, Run-out, Ball bearing, Dynamic and spectrum models, Imperfections of bearings

For the purpose to improve and to automate designing of high-speed spindle units (SU's), we have developed the mathematical models and software to estimate SU performance characteristics, including the run-out of spindles running on ball bearings. In order to understand better the mechanics of high-speed SUs, the dynamic interaction of ball bearings and SU, and the influence of the bearing imperfections and SU's operational conditions on the run-out, we have carried out computer simulation and experimental studies. Through the study of SU's, we have found out that run-out of SU can vary drastically with variation of rpm. The influences of rotation speed and of accuracy parameters of bearings on the SU accuracy have the greatest importance. The influence of bearing preload has a secondary importance. Comparison of the results of these studies has demonstrated adequacy of the models and software developed to the real SU's.

Manuscript received: December 3, 2004 / Accepted: November 10, 2005

1. Introduction

We can define accuracy of rotation of SU as stability or immobility of its spindle axis during rotation. Basically, accuracy is the value inverse to imperfection, and in practice, we usually check SU imperfection by checking its vibration and measuring spindle axis displacements (vibration amplitudes or run-outs). There are several reasons for spindle vibration,[1] among which we can point out imperfections of bearings,[2~4] spindle unbalances, disturbances caused by the drive or the motor,[1] etc. The vibration caused by unbalance is the most simple one, since it takes place at one frequency - the frequency of rotation, and can be improved by spindle balancing.[5] In this article, we investigate the run-out of SU's caused by the ball bearings. In other words, we study the imperfections of spindle rotation caused by the bearing imperfections. We define imperfection of spindle rotation (the inverse to the accuracy of rotation of SU) as the root-mean square sum of the frequency components of spectral decomposition of spindle axis vibrodisplacements, excluding the component (harmonic) at the speed of rotation, and define this sum run-out. We introduce such a measure of accuracy of rotation since it follows the method of its measurement in practice: the most detailed information about spindle rotation in practice we get by measuring its vibration with different types of sensors and representing the vibration in the form of a spectrum of vibrodisplacements with the spectrum analysers. Averaged summation of the spectrum amplitudes gives us a general measure of vibrodisplacements. Such a spectrum depends on disturbances (produced by imperfect bearings in our case) and elastic and damping properties of the structure. Our general purpose is to estimate the influence of these factors on SU spectrum of vibrodisplacements and, finally, to reduce as much as possible its root-mean-square amplitude (or the run-out) by the perfect design (choice) of SU structure.

2. Dynamic Model of High-Speed Spindle Units

Following the purpose stated above, we have developed a complex mathematical model of high-speed SU's,[1] one of whose elements is the dynamic model (Fig. 1).

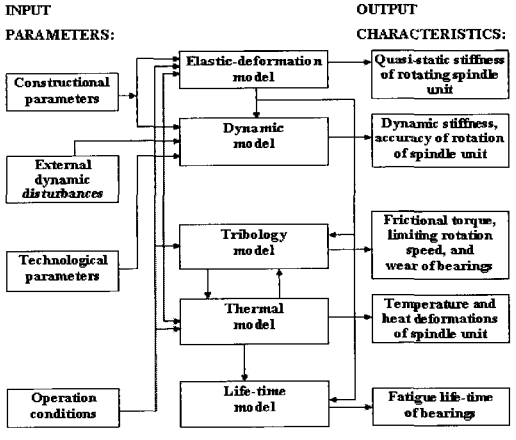

Fig. 1 Diagram of the complex model of spindle units

This model gives us an opportunity to estimate the following characteristics of SU dynamics:

1. Stiffness (compliance) in dynamics in the form of amplitude-frequency characteristic;
2. Accuracy in dynamics estimated by the amplitude-frequency spectrum of vibrodisplacements and run-out of spindle.

The structural and analytical diagrams used for the analysis of experimental high-speed SU are presented in Fig. 2 (a) and (b). We make the following basic assumptions:

1. We consider the SU to be a linear dynamic system having continuous and lumped parameters;
2. We assume the spindle to be an elastic beam of variable cross-section;
3. We assume that bearings have linear elastic and damping characteristics.

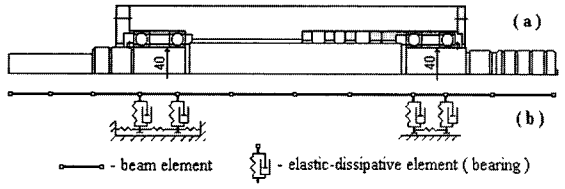

Fig. 2 Structural (a) and analytical (b) diagrams of the spindle unit

When representing the SU by the analytical diagram (Fig. 2b), we apply the finite element method (FEM).[6] We represent each spindle's element by a 2-node beam element, where each element has three degrees of freedom (radial, axial, and angular). We describe spindle dynamic displacements by a system of linear ordinary differential equations in the matrix form as follows:

$$M\cdot\ddot{\mathbf{X}} + B\cdot\dot{\mathbf{X}} + K\cdot\mathbf{X} = F(t) \tag{1}$$

where $\boldsymbol{X}(t)$ is the vector of nodal displacements; $\boldsymbol{F}(t)$ is the vector of nodal dynamic loads; **M**, **B**, and **K** are the matrices of SU's mass, damping, and stiffness; and t is time.

Assuming that damping forces in bearings are proportional to elastic forces[4], i.e. $\omega\cdot\mathbf{B} = \eta\cdot\mathbf{K}$ (where η is the damping coefficient, ω is the frequency of oscillation), and that dynamic loads have a harmonic characteristic, i.e.

$$F(t) = F_o\cdot e^{i\omega t} \tag{2}$$

and following Ref. 6, we express the complex vector of dynamical amplitudes $\boldsymbol{X}_o$ through the matrix of natural forms $\boldsymbol{V}$ and frequencies of oscillations ω_s (where s is the number of natural frequency) as follows:

$$X_o = V\cdot \mathrm{diag}\left(\frac{1}{[1+i\cdot\eta]\cdot\omega_s^2-\omega^2}\right)\cdot V^T\cdot F_o = W\cdot F_o \tag{3}$$

where $\boldsymbol{F}_o$ is the complex vector of amplitude nodal loads; **W** is the matrix of frequency functions; i is the imaginary unit. Thus, the modal matrix $\boldsymbol{V}$ has the properties of orthogonality[6], i.e.

$$V^T\cdot M\cdot V = E \text{ (unit matrix)} \tag{4}$$

$$V^T\cdot K\cdot V = \mathrm{diag}(\omega_s^2) \tag{5}$$

We derived equation (3) by the expansion of vibration-forced amplitudes into the series in terms of the eigenfunctions. The amplitude-frequency characteristics represented by equation (3) correspond to monoharmonic vibrodisturbance. In the case of polyharmonic vibrodisturbance produced by several bearings, we can derive the dynamic load as follows:

$$F(t) = \sum_p \sum_{k=1}^{N} \mathbf{F}_k(\omega_k)\cdot e^{i\omega_k t+\varphi_k} \tag{6}$$

where p is the number of bearings in SU; N is the number of spectrum harmonics to be considered; $\boldsymbol{F}_k(\omega_k)$ is the vector of nodal loads of the k-th harmonic; ω_k and φ_k are the frequency and phase of the k-th harmonic.

The hardware that we apply for measuring of spectrum of spindle vibrodisplacements gives us an opportunity to make a root-mean-square summation of vibrodisplacement harmonics, which is the frequency band to be checked $\Delta\omega_r$ (r = *1, 2, 3, ..., q*), where q is the number of frequency bands. The root-mean-square amplitude of vibrodisplacements of the vector $\boldsymbol{X}_o$ on the coordinate j in the frequency band $\Delta\omega_r$ (the double of which we term the run-out) can be determined as follows:

$$A_j(\Delta\omega_r) = \sqrt{\sum_p \left(\sqrt{\sum_{\omega_k\in\Delta\omega_r} [\mathbf{W}_{jn}\cdot\mathbf{F}_n(\omega_k)]^2}\right)^2} \tag{7}$$

where $\mathbf{W}_{jn}$ are the elements of the matrix of frequency function (3); $\boldsymbol{F}_n(\omega_k)$ is the k-th harmonic of the n-th component of vector of vibrodisturbances, and $\sum_{\omega_k\in\Delta\omega_r}$ denotes summation of all the harmonics ω_k, which enter into the frequency band $\Delta\omega_r$. We can use formula (7) to estimate the accuracy of rotation of SU in the frequency band to be checked $\Delta\omega_r$.

3. Model of Bearing Disturbances

High-speed ball bearings have several sources of disturbances, i.e. the forces, which produce the vibration of SU parts. These are:

1. Imperfections of macrogeometry of bearing's races, such as out-of-roundness, waviness, radial and axial run-outs, possible dents and scratches, etc.;
2. Imperfections of macrogeometry of the balls, which are similar to those of the races, plus possible differences of ball sizes;
3. Imperfections of microgeometry of races and balls, i.e. surface roughness (some of these imperfections protrude through the oil film generated between races and balls during normal operation and produce collisions);
4. Variation of bearing stiffness during rotation (the radial stiffness depends on the position of balls with respect to the radial force vector);
5. Heterogeneity of elastic properties of races and balls;
6. Lubricant contamination;
7. Motion of cage;
8. Unbalance of spindle and bearing misalignments, etc.

Table 1 Spectra of radial vibrodisturbances of ball bearings

Bearing's elements	Number of harmonics	Frequency of vibrodisturbances [Hz]	Amplitude of vibrodisturbances [N]
Outer ring	$\lambda = mz \pm 1$	$(\lambda \pm 1)\,\omega_o$	$K_R\cdot a_\lambda$
Inner ring	$\chi = kz \pm 1$	$\chi\cdot\omega_i \pm \omega_o$	$K_R\cdot a_\chi$
Outer and inner rings	$\lvert\lambda+\chi\pm1\rvert = mz$ $\lvert\lambda-\chi\pm1\rvert = kz$	$\lvert\lambda\cdot\omega_o - \chi\cdot\omega_i \pm \omega_o\rvert$ $\lvert\lambda\cdot\omega_o + \chi\cdot\omega_i \pm \omega_o\rvert$	$K_R\cdot\frac{\mathrm{ctg}(\tau)}{4\cdot\delta}\,a_\lambda\cdot a_\chi$
Balls (out-of-roundness)	$\xi = 2, 4, 6, \ldots$	$\xi\cdot\omega_b \pm \omega_o$	$K_R\cdot\frac{\sqrt{2}}{\sqrt{\pi z\cdot\cos(\tau)}}\,a_\xi$
Balls (out-of-diameter)	$\xi = 0$	ω_o	$K_R\cdot\frac{\Delta}{3\sqrt{2z}\cdot\cos(\tau)}$
Outer ring and balls (out-of-diameter)	$\xi = 0;\ \lambda = m$	$(\lambda \pm 1)\cdot\omega_o$	$K_R\cdot\frac{\mathrm{ctg}(\tau)\cdot\Delta}{3\pi\sqrt{2z}\cdot\delta}\,a_\lambda$
Inner ring and balls (out-of-diameter)	$\xi = 0;\ \chi = k$	$\chi\cdot\omega_i \pm \omega_o$	$K_R\cdot\frac{\mathrm{ctg}(\tau)\cdot\Delta}{3\pi\sqrt{2z\delta}}\,a_\chi$

Note: z is the number of balls in bearing; τ is the contact angle of bearing; δ is the axial clearance-tightness of bearing, (μm); K_R is the radial stiffness of bearing, ($N\cdot\mu m^{-1}$); ω_o, ω_i, ω_b are the rotation speeds of a bearing's cage relatively outer and inner rings, and of balls around their own axis, (Hz); ξ is the number of harmonics of Fourier-series expansion of ball radius; a_ξ is the amplitude of the harmonic ξ of ball radius; λ, χ, a_λ, a_χ are the numbers and amplitudes of harmonics of imperfections of outer and inner races; Δ is the allowance of out-of-diameter of balls, (μm); $k = 0, 1, 2, \ldots$; $m = 1, 2, \ldots$ are the coefficients.

However, when analyzing precision bearings of precision SU's operating in favorable conditions, we can neglect some of these

sources and keep first two sources. The theory of bearings having these imperfections is considered by Juravlev and Balmont.[7] Some of the results obtained are presented in Table 1, where spectra of radial vibrodisturbances generated by imperfect ball bearings are presented.

Table 1 interrelates two types of the spectra: the spectra of imperfections of ball bearing's races and balls (the input parameters represented by amplitudes of these imperfections $a_\lambda(\lambda)$, $a_\chi(\chi)$, and $a_\xi(\xi)$ and the spectrum of radial vibrodisturbances determined by the frequencies and amplitudes of harmonics (the output parameters), which are represented in two right columns of Table 1. The spectrum of angular vibrodisturbances coincides with the spectrum of radial ones and differs in amplitudes by the multiplier $0.5 \cdot D_m \cdot \mathrm{tg}(\tau)$, where D_m is the diameter of the circle, which goes through the centers of bearing's balls. Spectrum of axial vibrodisturbances of ball bearings having imperfections of macrogeometry is also considered in Ref. 7.

The amplitudes of imperfections $a_\lambda(\lambda)$, $a_\chi(\chi)$, and $a_\xi(\xi)$ have a particular physical sense. The subscripts and arguments λ, χ, and ξ notify numbers of harmonics of expansions of imperfections into Fourier series and attribute them to outer ring (λ), inner ring (χ), and balls (ξ). Here, first two profiles are the combinations of imperfections of races measured in three directions: transversal, radial, and axial, which can be designated by upper indexes (1), (2), and (3), respectively (Fig. 3).

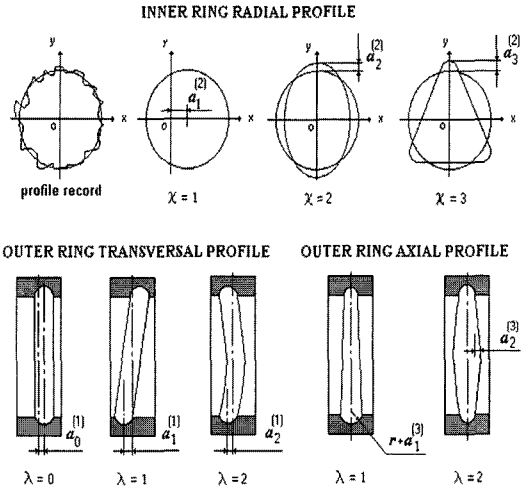

Fig. 3 Imperfections of macro-geometry of bearing's races

Thus, for example, $a_\lambda(\lambda)^{(1)}$ is the amplitude of the harmonic λ of bearing's outer race cross-section imperfection; $a_\lambda(\lambda)^{(2)}$ is the amplitude of the harmonic λ of bearing's outer race radial imperfection; $a_\lambda(\lambda)^{(3)}$ is the amplitude of the harmonic λ of bearing's outer race axial imperfection. These imperfections can be measured using the round-meter gauges of Taylor&Hobson Co. Here, the measurements of the axial and radial imperfection spectra should be made by the Talyrond instrument and the measurements of the cross-section imperfections - by the Talyserf instrument (both of them should be equipped by the Talydate facility for expansion of the traces by Fourier series). Summation of the components should be made as follows:

$$a_\lambda = \sqrt{\left[\frac{\cos(\tau)-1}{\cos(\tau)} a_\lambda^{(1)}\right]^2 + \left[a_\lambda^{(2)}\right]^2 + \left[\mathrm{tg}(\tau)\cdot a_\lambda^{(3)}\right]^2} \quad (8)$$

$$a_\chi = \sqrt{\left[\frac{\cos(\tau)-1}{\cos(\tau)} a_\chi^{(1)}\right]^2 + \left[a_\chi^{(2)}\right]^2 + \left[\mathrm{tg}(\tau)\cdot a_\chi^{(3)}\right]^2} \quad (9)$$

Representation of imperfections of races and balls by Fourier series has a clear mechanical sense: harmonics $a_{\lambda=2}$, $a_{\chi=2}$, and $a_{\xi=2}$ correspond to ovality of outer race, inner race, and balls (when averaged), respectively; $a_{\lambda=3}$, $a_{\chi=3}$, and $a_{\xi=3}$ - to triangularity, etc.; $a_{\lambda=1}$ and $a_{\xi=1}$ has no meaning; $a_{\chi=1}$ corresponds to eccentricity of the inner race with respect to rotation axis, i.e. to spindle unbalance (which is an imperfection of SU accuracy, not of the bearing); $a_{\xi=0}$ corresponds to averaged difference between diameters of balls.

The principal difficulty when simulating the ball bearing vibration spectrum results in inputting of the spectra of bearing imperfections. It looks to be impossible to measure and to input all the harmonics of races and balls individually. In order to avoid it, we can use some extrapolation based on results of measurements of races and balls, and represent the spectra of imperfections by following hyperbolic functions:

$$a_\chi = \frac{\alpha_2}{\chi^{\beta_2}} \quad ; \quad a_\lambda = \frac{\alpha_1}{\lambda^{\beta_1}} \quad ; \quad a_\xi = \frac{\alpha_3}{\xi^{\beta_3}} \quad (10)$$

Here, the coefficients α and β can be determined as the regressive factors to be derived by statistical treatment of the results of measurements of real races and balls. The results of such measurements and treatment for some precision bearings are presented in Table 2.

Table 2 Regressive coefficients α and β

Bearings	Outer ring		Inner ring	
	α_1 [μm]	β_1	α_2 [μm]	β_2
Roller bearing 3011 (FAG)	0.366	1.02	0.145	0.971
Roller bearing 2-3182111 (GPZ, Russia)	2.470	2.25	0.488	2.02
Ball bearing 2-36106K6 (GPZ, Russia)	0.380	1.50	0.350	1.90
Ball bearing 6-206 (GPZ, Russia)	1.223	1.75	0.95	2.06
Ball bearing 2-206 (GPZ, Russia)	1.568	2.46	0.889	2.01

The coefficients α_1, α_2 depend on the accuracy of bearing's parts machining, and the coefficients β_1, β_2 on the type of technology of races and balls machining. More accurate are the bearings, the lower are α's. The regressive curves approximating the spectrums of the bearings presented in Table 2 are shown in Fig. 4.

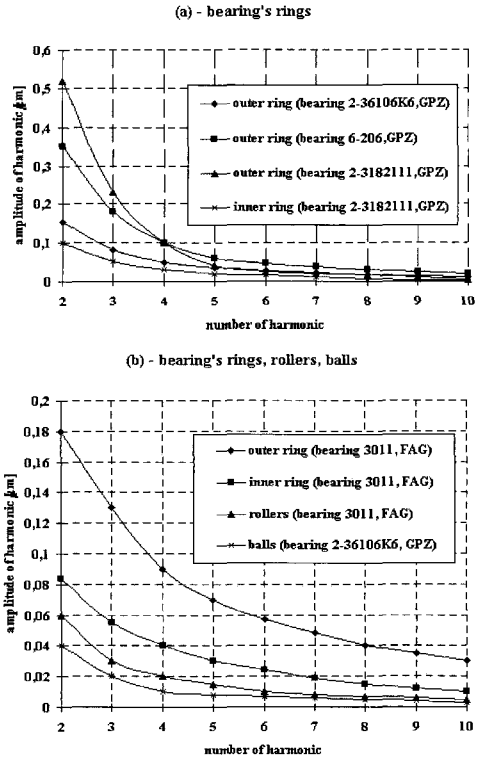

Fig. 4 Regressive curves of the spectrums of bearing's elements

The effect of ball bearing assembly in SU (misalignments of rings) on SU vibration was studied in Ref. 8.

4. Algorithm of Simulation

The program flowchart we used for the simulation of SU dynamics is presented in Fig. 5.

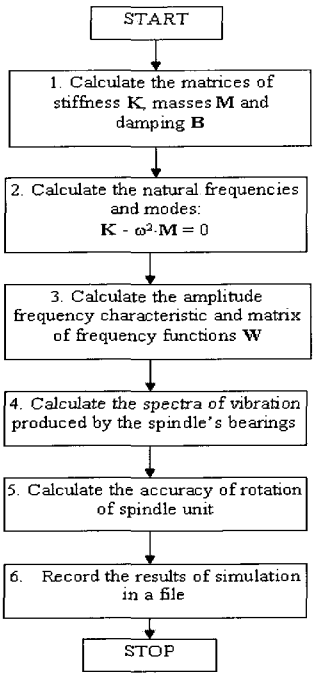

Fig. 5 Algorithm diagram of the rotational accuracy problem solution

In Fig. 5, we are calculated the matrices of stiffness **K**, masses **M**, and damping **B** of SU dynamic system in block 1. For estimation of eigenvalues, we apply the Jacobi method in block 2 and thus determine the natural frequencies and modes of SU oscillation. We estimate the SU dynamical compliance in the form of amplitude-frequency characteristics by calculating the matrix of frequency functions **W** in block 3. We simulate the spectra of vibrodisturbances produced by the bearings in block 4. We solve the problem of SU forced oscillation in block 5. Hence, we obtain the radial and axial spectra of spindle vibrodisplacements and the radial and axial run-outs (which are the doubled root-mean-squares of spindle axis radial and axial vibrodisplacements when ignoring the component at the rotation frequency caused by the unbalance and misalignment of bearings' rings). We record the results of simulation in block 6 and use in the further analysis.

5. Analysis of Run-out of Spindle Unit

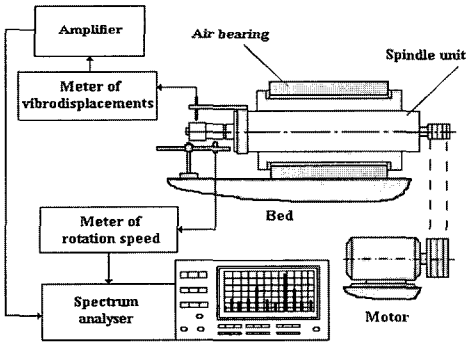

Fig. 6 Layout of the experimental rig

In order to make experimental study of run-out of SU, we used a special test rig (Fig. 6). The precision high-speed SU (Fig. 2a) running on the precision ball bearings (ABEC 9 class, USA Standard) was mounted in an aerostatic bearing to isolate the SU from the bed and the drive.

The spindle vibrodisplacements were measured by the contactless sensor WSG 69-5 fixed at the SU's housing and the amplifier WSM-6983 (Roitlinger Co.). After SU acceleration to the highest rpm, we were unswitching the belt of the drive, breaking the drive motor, and then, the measurements were carried out. We were analyzing the signal from the amplifier using the spectrum analyser of model 2031 (B&K Co.). Using the special method for data processing[9], we increased the accuracy of measurements of the spindle displacements up to 0.1 μm.

The results of the measurements had two kinds of errors: a) the error caused by the imperfections of shape of spindle mandrel; b) the error caused by the discontinuity of magnetic conductivity of mandrel's material. We corrected these errors using the results of the mandrel profiling by the Talyrond instrument and the technique presented in Ref. 9.

The results of the measurements and of the simulation of SU vibration are presented in Fig. 7. We can see three resonance frequencies. We attribute the first one at n_1 = 5,200 rpm to the coincidence of the vibrodisturbance harmonic $z{\cdot}\omega_o$ (where z is the number of balls of the bearing and ω_o is the bearing's cage rotation frequency) and the SU first natural frequency f_1 = 650 Hz. We attribute two other resonance frequencies, n_2 = 12,000 rpm and n_3 = 18,000 rpm to the coincidence of the vibrodisturbance harmonics caused by the outer ring triangularity (3-rd harmonic of the outer ring's race imperfection) and by the outer ring ovality (2-nd harmonic of the outer ring's race imperfection) and the SU first natural frequency.

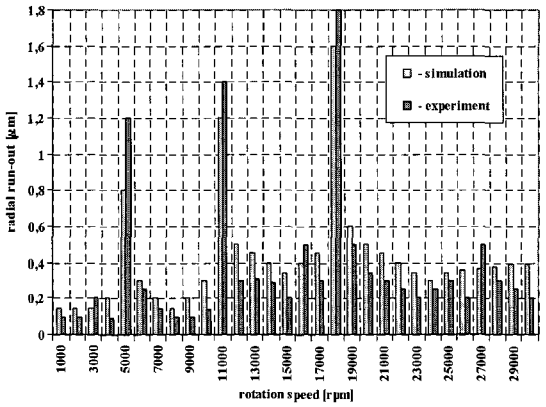

Fig. 7 Run-out of the spindle related to rpm

The SU radial run-out at low rpm (n < 2,000 rpm) is about 0.1-0.2 μm, which is practically equal to the run-out of the precise bearings. But at resonance rpm, the SU run-out increases up to 1.0-1.8 μm. When comparing the results of computer simulation with that obtained by experimental measurements, we can see that the error of resonance rpm simulation does not exceed 10-12 %, and the error of estimation of amplitudes of vibrodisplacements does not exceed 20-25 % at the nonresonant mode and 20-30 % at the resonant mode. In order to examine the influence of bearing preload on the SU run-out, we made the simulation and experimental studies of a SU having variable preload of ball bearings (Fig. 8).

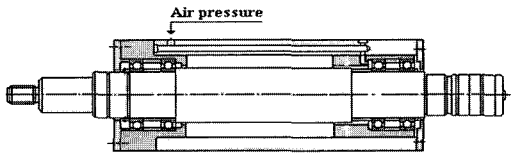

Fig. 8 Experimental high-speed spindle unit

The dependence of SU radial accumulative run-out in the frequency band of 24,000 rpm (as the root-mean-square amplitude of vibrodiplacements, which is the frequency band of 24,000 rpm) on the bearing preload is presented in Fig. 9.

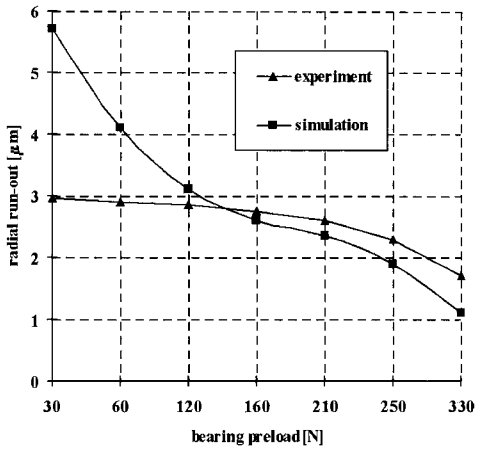

Fig. 9 Accumulative run-out of the spindle related to bearing preload

We can see that increasing of preload from the light preload of 120 N up to the heavy preload of 330 N results in the decrease of the run-out by 26 %, but in the increase of temperature of the front bearing's outer ring by 32 % at the same time (Fig. 10).

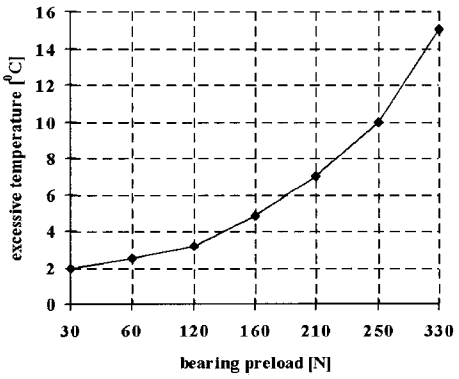

Fig. 10 Experimental temperature of the front bearing related to bearing preload

Under very low preload (lower than 60 N), simulation shows radical growth of the run-out, but in practice, it keeps steady; thus, it follows that under very low preload of bearings, the theory we use does not work perfectly well. However, at the medium (working) preload of 180-220 N, the SU run-out increase in the resonant mode does not exceed 15 % and this agrees with the theory well enough. The position of resonance peaks at the spectrum of SU vibrodisplacements remains practically constant and independent from spindle rpm, since the SU first natural frequency changes within 5-6 % only, when the preload changes within their medium range. In the nonresonant mode, an increase of bearing preload from light to heavy brings to the change of the run-out within 8-10 % only.

6. Conclusions

The results obtained are summarized as follows:

1. Having a purpose to improve quality of designing of high-speed SU's on rolling bearings, we have developed a SU dynamic model, which is one of the elements of SU complex model incorporating elastic-deformation, thermal models, and model of bearing lifetime. We represented the dynamic model developed as software for analysis of SU rotation accuracy at designing. The dynamic model incorporates the model of SU stiffness/compliance in dynamics in the form of amplitude-frequency characteristic, and the model of SU rotation accuracy estimated by the amplitude-frequency spectrum of vibrodisplacements and the run-out of spindle. The dynamic model is based on the application of beam type finite element analytical diagrams of SU's. The usage of beam type diagrams allows us to apply the universal SU's analytical diagrams for the solution of problems of statics, dynamics, and heat conduction, which is of great importance for practical realization of our complex approach to estimation of different characteristics of SU in designing. The theoretical and experimental studies showed that the theory is close to reality, and the models and software developed can be applied for SU's designing and development.
2. When studying the particular SU's by means of simulation and experimental measurements, we have found out that the run-out of the SU can vary drastically with variation of rpm. We determined the spindle run-out increase from 0.2-0.4 μm at low rpm to 1.0-1.8 μm at high rpm and at resonant modes of operation. The influence of rotational speed and of bearings' accuracy parameters on the run-out has the greatest importance. The influence of bearing preload on the SU accuracy has a secondary importance, and variation of bearing preload does not bring to significant variation of SU rotation accuracy.

ACKNOWLEDGEMENT

This work was supported by grant No. RTI04-01-03 from Regional Technology Innovation Program of the Ministry of Commerce, Industry and Energy(MOCIE).

REFERENCES

1. Zverev, I. A. and Push, A. V., "Spindle Units: Quality and Reliability at Designing," Moscow State University of Technology Press, 2000.
2. Tamura, A. and Shimizu, H., "Vibration of a rotor based on ball bearings," Journal of Manufacturing Science and Engineering, Vol. 41, pp. 763-775, 1967.
3. Tamura, A., "Vibration caused by ball diameter difference in ball bearings," Journal of Manufacturing Science and Engineering, Vol. 44, pp. 229-234, 1968.
4. Balmont, V. B. and Zverev, I. A., "Model of spindle vibration caused by ball bearings," Journal of Vibration Engineering, Vol. 3, pp. 149-157, 1989.
5. Venkatraman, V., "Analysis of spindle running accuracy," Journal of Machine and Production Engineering, Vol. 12, pp. 146-150, 1975.
6. Segerlind, L. J., "Applied Finite Element Analysis," John Wiley & Sons Inc., 1976.
7. Juravlev, V. F. and Balmont, V. B., "Mechanics of ball bearings of gyroscopes," Moscow: Mashinostroenie, Russia, 1985.
8. Pozdnyak, E. I., "Estimation of vibration caused by rolling bearing's imperfections," Journal of Machinary Manufacture and Reliability, Russian Academy of Sciences, Allerton Press Inc., Vol. 5, pp. 17-23, 1976.
9. Danilchenko, J. M., "Experimental research of accuracy of rotation of spindles running on ball bearings," Ph. D. thesis, Moscow Research Institute of Machine Tools, Russia, 1986.